Chaos Synchronization in the Belousov-Zhabotinsky Chemical Reaction by Adaptive Control Scheme

LI, Yan-Ni(李艳妮) CHEN, Lan(陈兰) CAI, Zun-Sheng*(蔡遵生)
ZHAO, Xue-Zhuang(赵学庄)
Department of Chemistry, Nankai University, Tianjin 300071, China

The adaptive synchronization scheme proposed by John and Amritkar was employed into the Belousov-Zhabotinsky (BZ) 4-variable-Montanator model system. By the parameter adjustment, chaos synchronization has been obtained. Through calculating the transient time, the optimal combination of the stiffness constant and damping constant was obtained. Furthermore, the relationships among the transient time, conditional Lyapunov exponents, the stiffness constant and damping constant were discussed. Also, the BZ system with the adaptive synchronization scheme might be used for the communication purposes.

Keywords chaos, synchronization, Belousov-Zhabotinsky chemical reaction, adaptive control scheme

Introduction

Recently synchronization between two structurally identical (but initial states maybe not identical) chaotic systems has attracted a great deal of interest for its potential applications.[1-5] Various strategies have been applied to carry out the synchronization. As a whole, synchronization strategies can be classified into two categories: one is the state variable regulation,[6-8] the other is the operation parameter adjustment.[9,10] On the variable regulations, the most representative strategy is the Pecora-Carroll (PC) method.[6] In this method, a chaotic system, whose largest Lyapunov exponent is positive, is divided into a drive subsystem and the remainder subsystem whose Lyapunov exponents are all negative. The chaotic system is now coupled with a driven system, in which everything is the same as that of the remainder subsystem in the chaotic system except for the initial values of state variables. Thus the trajectories from the driven subsystem can be synchronized with that remainder subsystem. Nevertheless, due to the requirement of properly dividing the system, this method is not always feasible. On the parameter adjustment, a chaos controlling method of OGY[9] (Ott, Grebogi and Yorke) has been used to synchronize structurally identical chaotic systems. It was shown that by applying small, judiciously chosen, temporal-parameter perturbation to one of the chaotic systems, the trajectory around a chaotic trajectory of the other system could be stabilized and synchronization of the two systems was achieved. The OGY method requires a permanent computer monitoring of the state of the system and deals with the Poincare map of the trajectory in phase space to evaluate the changes of the parameter.

In 1994, another convenient parameter regulation scheme for synchronizing the evolution of a chaotic system with a desired chaotic trajectory of another system through adaptive control was proposed by John and Amritkar.[11] It is based on the idea of adaptive control suggested by Huberman and Lumer (HL),[12,13] which utilizes an error signal proportional to the difference between the goal output and the actual output of the system. This error term is now associated with a term which is proportional to the change of the parameters of the system, so that the parameters are adjusted to reduce the error to zero. Since the approach is merely to introduce changes in the system parameters, all the state variables of the system evolve freely. Also, a detailed knowledge of the underlying at-

* E-mail: caizunsh@nankai.edu.cn; Tel: 022-23509201
Received November 27, 2001; revised March 22, 2002; accepted April 23, 2002.
Project supported by the Research Foundation of Nankai University to homecoming scholars.

tractor of the dynamics is not necessary. The effectiveness of this approach has been demonstrated by the well-known Lorenz and Rössler systems.[11] In this paper the approach by modulating the system parameter (flow-rate) is employed into a real chemical reaction system model: 4-variable Montanator model[14], and the identical synchronization (IS), namely, the complete coincidence of the states between two systems was obtained successfully.

Adaptive control scheme[11]

A general description of the control procedure is as follows: For a general N-dimensional autonomous dynamical system: $\dot{u} = f(u, \mu)$, where $u = (u_1, u_2, \cdots u_N)$ are state variables and $\mu = (\mu_1, \cdots, \mu_k)$ are operation parameters. The system generating a desired trajectory is viewed as the target system and the controlled system as the response system. In order to synchronize the variable u of the response system with the variable u^* of the target system, a small perturbation in the parameter μ_i is introduced:

$$\mu_i = -\varepsilon(u - u^*)_j \operatorname{sgn}\left[\frac{\partial f_j}{\partial \mu_i}\right] - \delta(\mu_i - \mu_i^*) \quad (1)$$

where ε and δ are called the stiffness constant and the damping constant, respectively, which mean that a balanced relationship should exist between them in order to achieve synchronization, u_j denotes the state variable whose evolution equation includes the adjustable parameter μ_i, and μ_i^* is the value of the parameter μ_i in the target system. The function $\operatorname{sgn}(x)$ denotes the sign of x. Frequently, except for a particular μ_i, other parameters in the response system are kept the same as those in the target system. In certain ranges of ε and δ, the response system can be forced onto the desired trajectory of the target system.

Model for the BZ reaction

Simulations are performed using a 4-variable Montanator model after Gyorgyi and Field. The kinetics is described by differential equations:

$$\begin{aligned} d[Br^-]/dt = &- k_{D1}[H^+][Br^-][HBrO_2] - k_{D2}\cdot \\ &[BrO_3^-][H^+]^2[Br^-] + k_{D7}[Ce(IV)]\cdot \\ &[BrMA] + k_{D8}[MA\cdot]_{QSS}[BrMA] + k_f\cdot \\ &([Br^-]_{mf} - [Br^-]) \end{aligned}$$

$$\begin{aligned} d[HBrO_2]/dt = &- k_{D1}[H^+][Br^-][HBrO_2] + k_{D2}\cdot \\ &[BrO_3^-][H^+]^2[Br^-] - 2k_{D3}\cdot \\ &[HBrO_2]^2 + 0.5k_{D4}[H^+]([Ce]_{tot} - \\ &[Ce(IV)])[BrO_2\cdot]_{est} - 0.5k_{D5}\cdot \\ &[HBrO_2][Ce(IV)] + k_f([HBrO_2]_{mf} - \\ &[HBrO_2]) \end{aligned}$$

$$\begin{aligned} d[Ce(IV)]/dt = &\ k_{D4}[H^+]([Ce]_{tot} - [Ce(IV)])\cdot \\ &[BrO_2\cdot]_{est} - k_{D5}[HBrO_2][Ce(IV)] - \\ &k_{D6}[MA][Ce(IV)] - k_{D7}[Ce(IV)]\cdot \\ &[BrMA] + k_f([Ce(IV)]_{mf} - \\ &[Ce(IV)]) \end{aligned}$$

$$\begin{aligned} d[BrMA]/dt = &\ 2k_{D1}[H^+][Br^-][HBrO_2] + k_{D2}\cdot \\ &[BrO_3^-][H^+]^2[Br^-] - k_{D3}[HBrO_2]^2 \\ &- k_{D7}[Ce(IV)][BrMA] - k_{D8}\cdot \\ &[MA\cdot]_{QSS}[BrMA] + k_f([BrMA]_{mf} - \\ &[BrMA]) \end{aligned}$$

where $[MA\cdot] = \{-k_{A15}[BrMA] + \{(k_{A15}[BrMA])^2 + 8k_{A13}k_{A18}[MA][Ce^{4+}]\}^{0.5}\}/(4k_{A18})$

$$[BrO_2\cdot]_{est} = [BrO_2\cdot]_{EQ} = (k_{A7}[HBrO_2]/k_{A8})^{0.5}$$

and $k_{A15} = 2.4 \times 10^4\ L\cdot mol^{-1}\cdot s^{-1}$, $k_{A13} = 0.3\ L\cdot mol^{-1}\cdot s^{-1}$, $k_{A18} = 3.0 \times 10^9\ L\cdot mol^{-1}\cdot s^{-1}$, $k_{A7} = 0.858\ s^{-1}$, $k_{A8} = 4.2 \times 10^7\ L\cdot mol^{-1}\cdot s^{-1}$, the subscript mf means mixed-feed, k_f is the flow-rate. The parameters and the initial conditions used are the same as Ref. 14. The Montanator shows Period (P)-Chaos (C) series,[15] P1-C1-P2-C2-P3-C3-P4-, in which an appropriate value of k_f can be chosen for any prescribed dynamic behavior. In this paper three chaotic regions have been investigated. In every chaotic region, two flow-rates are chosen in the investigation, *i.e.*, C1 region: $6.16 \times 10^{-4}\ s^{-1}$, $6.17 \times 10^{-4}\ s^{-1}$; C2 region: $5.94 \times 10^{-4}\ s^{-1}$, $5.95 \times 10^{-4}\ s^{-1}$; C3 region: $5.71 \times 10^{-4}\ s^{-1}$, $5.74 \times 10^{-4}\ s^{-1}$.

Numerical results

As mentioned, the adaptive control scheme has been applied to Lorenz and Rössler systems. In either system, the controlled parameter exists only in one of the state variable evolution equation. However, in the BZ-4-variable-Montanator model, the unique adjustable parameter, the flow-rate (k_f), occurs in all of the four state variable

evolution equations, which may enhance the difficulty and complexity of synchronization by the possibly different requirements from four state variables on the flow-rate. Therefore, in terms of the principle of adaptive control, the operation rule for the parameter k_f is constructed as follows:

$$k_j = -\varepsilon\left\{\sum_{i=1}^{4}(Y_i - Y_i^*)\mathrm{sgn}\left[\frac{\partial Y_i}{\partial k_f}\right]\right\} - \delta(k_f - k_f^*) \quad (2)$$

where Y_i^* ($i = 1, 2, 3, 4$) is the Y_i variable of the desired chaotic system, in which $Y_1 \equiv [Br^-]$, $Y_2 \equiv [HBrO_2]$, $Y_3 \equiv [Ce^{4+}]$, $Y_4 \equiv [BrMA]$, and k_f^* is its flow-rate. An obvious distinction between Eqs. (1) and (2) is the construction of four pairs of variable difference into the rule because in this 4-variable model parameter k_f occurs in every evolution equation.

In the process of simulation, the first 6.0×10^4 steps have been neglected so as to avoid the transient effect. Two sets of simulations were performed with running lengths of 5.0×10^5 and 2.0×10^6 iterations, respectively. The result shows that the longer the integration time, the more combinations of ε and δ for achieving synchronization will be, but in some of the combinations quite large transient time will be required and no practical importance. Furthermore, our main goal is to investigate the relationship between the average transient time and ε, δ, and to explore the optimal combination of ε and δ. Therefore, computational time is set at 5.0×10^5 steps, which is long enough to scan possible significant synchronizations, and yields the maximum integration length (T_{max}) of 1.75×10^4 s.

Both of the identical systems, with the same structure and parameter values but different initial state variable values, and nonidentical systems, with the parameters which were initially different in two structurally identical systems were investigated. Our numerical results show that it is possible to synchronize the response system with the desired chaotic orbit in both cases. Compared with nonidentical systems, identical systems are more subject to be synchronized (data not shown). The results for nonidentical systems are presented in Fig. 1, that is, the plots of evolution time versus the variable difference ($Y_1 - Y_1^*$) and parameter difference ($k_f - k_f^*$). Other variable differences have the same behaviors (results not shown). The deviations decrease with time and the trajectory of the response system finally synchronizes with that of the target system.

The synchronization efficiency was investigated in terms of the transient time τ, which is defined as the time taken in order that the distance $d(\tau)$ in the phase space between the orbits of the two systems is of the order of assumed precision, *i.e.*, $d(\tau) < \eta$, where $d(\tau)$ is the average distance as ΔX^{12} in Ref. 16 and $\eta = 10^{-10}$.[16] For a higher accuracy or lower η, τ will be longer, but qualitative synchronizing features remain unchanged. The synchronization domain is defined as the ranges of ε and δ over which τ is finite. For the values of each pair of ε and δ, the average transient time $\bar{\tau}$ is the average of NI = 100 independent runs with randomly chosen initial concentration differences from $(Y_i)_0$: $(-0.5, 0.5) \times 10^{-2} \times (Y_i)_0$.

Fig. 2 shows the average transient time τ as a function of δ under certain values of ε, and the interplay of stiffness and damping constants is clearly seen. With the smaller ε ($\varepsilon = 1, 2, 3$) (Fig. 2a), $\bar{\tau}$ decreases with the increasing of δ, then there appears a flat section of small $\bar{\tau}$. Continue increasing δ, $\bar{\tau}$ increases sharply with δ. When δ exceeds the δ_{max} shown in the plot, $\bar{\tau}$ tends to infinity. In a word, there is a synchronization domain (δ_{min}, δ_{max}) in the plot of δ-$\bar{\tau}$, and $\bar{\tau}$ diverges near the domain boundary δ_{min} and δ_{max}. At $\varepsilon = 4.0$, some novel features emerge. The synchronization domain now contains two segments (Fig. 2b). For smaller δ of the first segment, $\bar{\tau}$ ascends gradually, while for larger δ of the second segment, $\bar{\tau}$ descends inch by inch, then levels off. The middle blank section of δ means that no finite $\bar{\tau}$ is attained. When ε is increased to 5.0, the plot changes again (Fig. 2c). For further high strength of ε (25—50), the plots of $\bar{\tau}$-δ show the same form in Figs. 2d, 2e and 2f, but they are different from Figs. 2b and 2c. In the range of even larger ε (100—200) (Fig. 2g), the same behavior exists, and the length of the flat section increases with the increasing of ε.

Considering the influence of flow-rates on $\bar{\tau}$ for this 4-variable Montanator model, the most efficient combination of ε and δ is $\varepsilon = 2.0$ and $\delta = 4.5 \times 10^{-2}$, respectively, which means that under this particular combination, the shortest $\bar{\tau}$ is available. The results in Fig. 2 are for $k_f = 5.71 \times 10^{-4}\ s^{-1}$ and $k_f^* = 6.16 \times 10^{-4}\ s^{-1}$, *i.e.*, the two flow-rates belong to C3 and C1 region, respectively. In addition, at the same k_f^* above, simulations are also performed in other several situations: (1)

$k_f = 5.94 \times 10^{-4}\ s^{-1}$ (C2 region); (2) $k_f = 6.17 \times 10^{-4}\ s^{-1}$ (C1 region); (3) $k_f = 6.16 \times 10^{-4}\ s^{-1}$ (C1 region). In the last situation, different initial values for the state variables are used in the response and target systems. No matter the two flow-rates are the same exactly, or they are slightly different but in the same chaotic region, or they are in entirely different chaotic region, the similar behaviors have been observed. In every situation, the most efficient combination is $\varepsilon = 2.0$ and $\delta = 4.5 \times 10^{-2}$. Only small difference exists among $\bar{\tau}$.

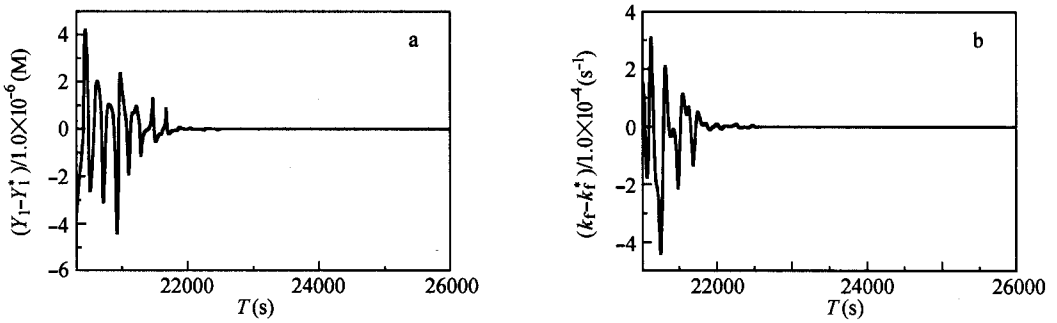

Fig. 1 Differences of corresponding state variable and parameter between the response and the target system. The adjustment starts at T = 21000 s, that is, after 6×10^4 steps. (a) $(Y_1 - Y_1^*)$-T; (b) $(k_f - k_f^*)$-T.

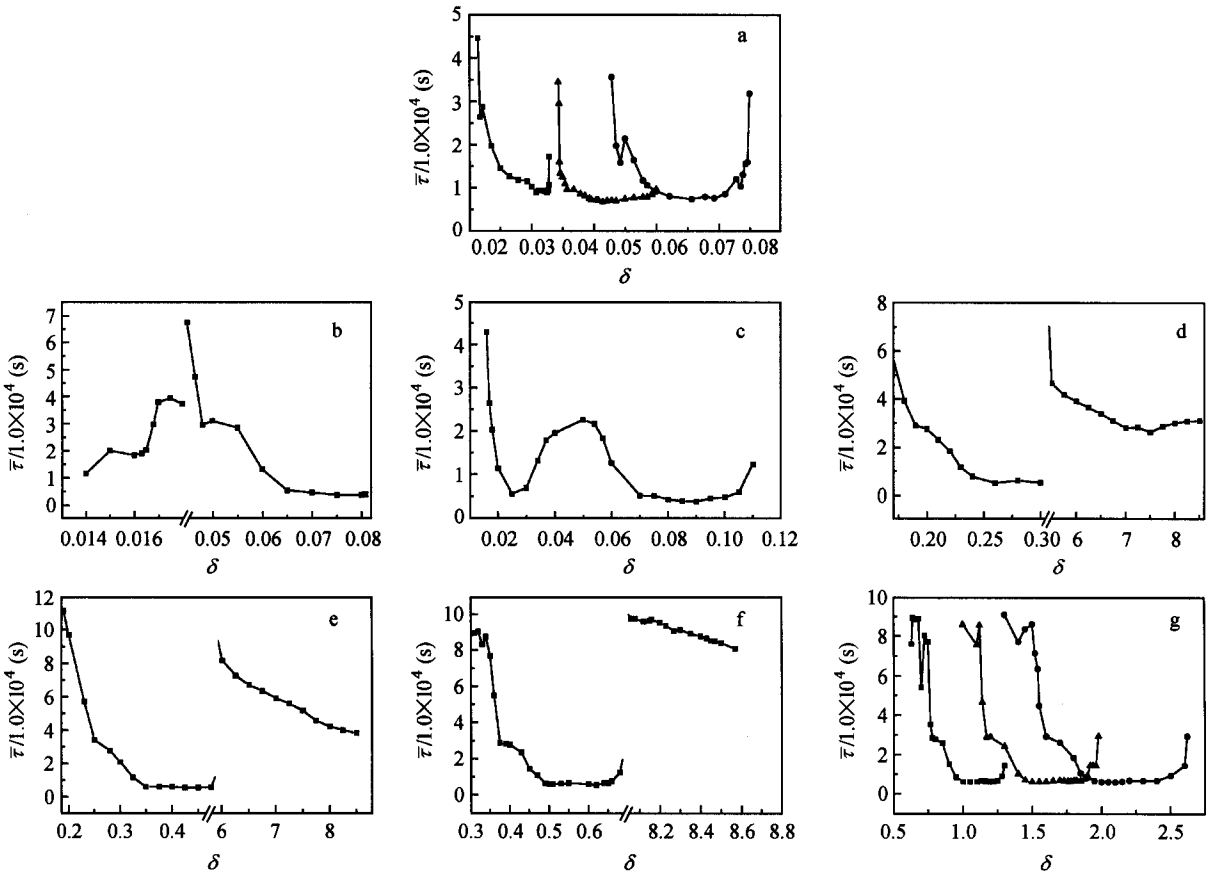

Fig. 2 Plots of average transient time ($\bar{\tau}$) as a function of damping constant δ at distinct stiffness constants ε. (a) $\varepsilon = 1.0$ (square), 2.0 (triangle), 3.0 (dot); (b) $\varepsilon = 4.0$. The break of the X-axis means $\bar{\tau}$ is infinite when ε lies in this range; (c) $\varepsilon = 5.0$; (d) $\varepsilon = 25.0$; (e) $\varepsilon = 35.0$; (f) $\varepsilon = 50.0$; (g) $\varepsilon = 100.0$ (square), 150.0 (triangle), 200.0 (dot).

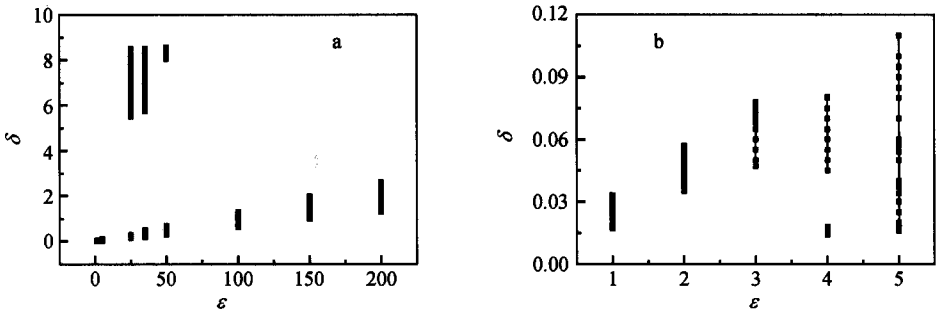

Fig. 3 Effective ranges of damping constant δ versus distinct stiffness constant ε. (b) is the enlargement of (a) ε of (1.0—5.0).

Fig. 3 shows the plot of ε-δ, in which Fig. 3b is the enlargement of Fig. 3a at $\varepsilon = 1$—5. It can be seen that with the increase of ε, the effective domain of δ is enlarged in general except for the cases of two segments, in which one segment is enlarged, and the other is reduced. In Fig. 3b, essentially only one segment appears for each ε, except for $\varepsilon = 4$, there are two segments, but the segment at lower δ is short and maybe not significant for further discussion. Although the flow-rate of the response takes other values as mentioned above, the same behavior can be obtained.

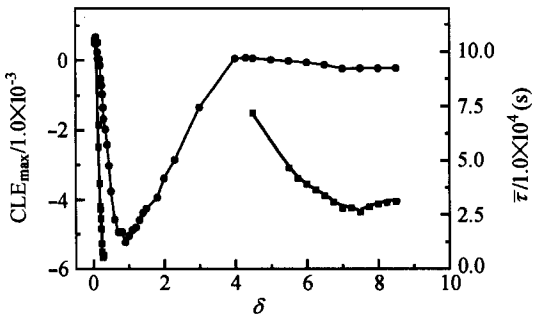

Fig. 4 Plot of maximum conditional Lyapunov Exponent (CLE_{max}) and the average transient time $\bar{\tau}$ versus the damping constant δ at $\varepsilon = 25.0$. The solid line with dots denotes δ vs. CLE_{max}, while the solid line with squares denotes δ vs. $\bar{\tau}$.

In addition, the stability of response system was investigated by studying the maximum conditional Lyapunov Exponents (CLE_{max}) through the method of Wolf *et al.*[17] Although Carroll and Pecora *et al.*[18] recently presented that there are four other criteria for high-quality synchronization, for the reason discussed more detail in Conclusions, CLE_{max} is used as the working criteria here. Fig. 4 shows the plot of CLE_{max} and $\bar{\tau}$ versus δ under the same ε. Indeed $\bar{\tau}$ is not finite when $CLE_{max} > 0$, and the critical value of δ is determined by the condition of $CLE_{max} = 0$. However, it is noticed that as δ in the range of 0.35—4.5, in spite of the negative CLE_{max}, $\bar{\tau}$ is not finite. In Ref. 6 it was pointed out that $CLE_{max} < 0$ in the response system is not a sufficient but a necessary condition. Therefore, although a negative value of CLE_{max} would signal that the orbits of response system starting from different initial conditions coalesce into the same final orbits, and thus synchronization ensues, which is not always the case. However, so long as CLE_{max} is negative and finite $\bar{\tau}$ is attained, the more negative the CLE_{max} is, the smaller $\bar{\tau}$ is.

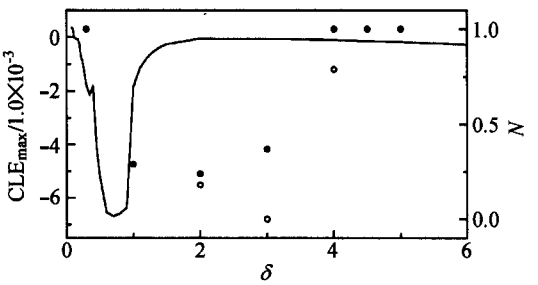

Fig. 5 Plot of maximum conditional Lyapunov Exponent (CL_{Emax}) and N (N = NS/NI) versus the damping constant δ at $\varepsilon = 25.0$. The solid line denotes δ vs. CLE_{max}, while the discrete makers denote δ vs. N. Circles and dots denote the results of running 5.0×10^5 and 2.0×10^6 iterations, respectively. Where only dots are shown, they coincide with circles.

On the other hand, for δ in the range of 0.35—4.5, though $\bar{\tau}$ is not finite, which does not mean that no synchronization is achieved under anyone of the possible initial conditions. Thus the fraction N = NS/NI is calculated (Fig. 5). NS is the number of runs for which synchronization is attained with the required precision and

within the maximum integration length (T_{max}) chosen above, and NI is 100 which is the number of total independent runs with randomly chosen initial conditions. At given ϵ and δ, $N = 0$ means that no synchronization is attained for any of the runs performed, following that $\bar{\tau}$ is longer than T_{max}. From Fig. 5 it can be seen that in this δ range, as T_{max} increases, N tends to 1, *i.e.*, synchronization can still be achieved but with a lower efficiency.

Application to communication

The greatest potential application of synchronization is in the field of secure communication. Here the possibility of using chaos synchronization to secure communication by a chemical reaction transmitter-receiver system was investigated, because this type of communication maybe one of the foundations in signal transition of living phenomena. In the following it was shown that introducing the adaptive control scheme in the BZ system could be used for communication.

The process of communicating a binary valued bit stream by the adaptive control scheme in BZ system is given in Fig. 6. The square waves with different duration time are generated for the binary 0 and 1. Considering the average transient time, each binary 1 state lasts for 175 s and each binary 0 state lasts for 3325 s. The parameter k_f^* of the transmitter is switched between $6.16 \times 10^{-4}\ s^{-1}$ and $6.20 \times 10^{-4}\ s^{-1}$ (Fig. 6a). The variation of k_f in the receiver is shown in Fig. 6b. In Fig. 6b there are obvious signal responses in the receiver system corresponding to what comes from the transmitter. It should be noted that because the transient time is quite long in BZ system, the signal transfer pace has to be slow. In addition, for either binary 1 state or binary 0 state, the length of duration times can influence the signal recovery significantly.

Conclusions

The adaptive control scheme has been employed to the BZ chemical reaction systems and the chaos synchronization has been achieved. According to the characteristic of the specific chemical system, a perturbation equation for the operation parameter has been constructed. The efficiency of the combinations of stiffness constant ϵ and damping constant δ has been investigated based on the average transient time $\bar{\tau}$. The results show that there exists optimal combinations of ϵ and δ. And the greater the value of ϵ is, the larger the domain of δ is. For a given ϵ, the change of $\bar{\tau}$ versus δ is complicated. The occurring of synchronization can partly be explained by the CLE_{max} of the response system as follows: so long as $CLE_{max} \geqslant 0$, no synchronization is attained, however for $CLE_{max} < 0$, there are certain possibilities to achieve synchronization. In Ref. 18 there are five criteria for identifying high-quality synchronization in the presence of noise. In this paper no noise is introduced specifically, thus criterion 1, that is, CLE_{max}, may be proper to be used here. On the other hand, it is essential to consider the requirement of all eigenvalues of the Jacobian matrix with negative real parts at all points along the driving trajectory. Also, from this numerical investigation, it is possible to have positive eigenvalues occasionally at certain points along the trajectory for some initial conditions, although the CLE_{max} is negative. Further investigation on this phenomenon is needed.

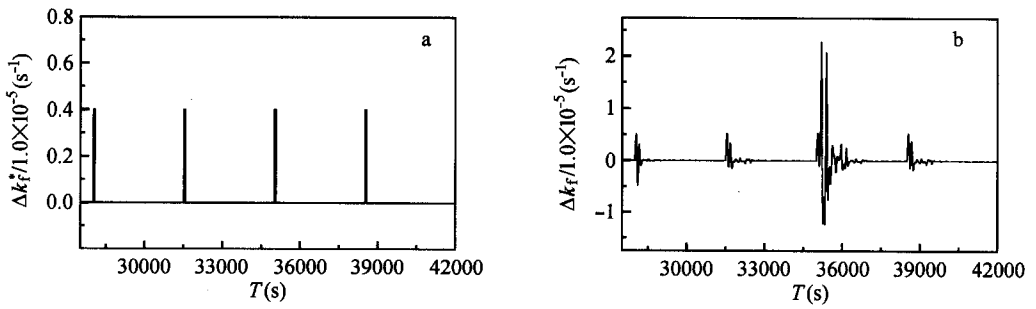

Fig. 6 Process of communicating a binary valued bit stream by adaptive control scheme in the BZ-4-variable-Montanator-Model. (a) Δk_f^* denotes the variation of k_f^* in the transmitter; (b) Δk_f denotes the variation of k_f in the receiver.

References

1 Cuomo, K. M.; Oppenheim, A. V. *Phys. Rev. Lett.* **1993**, *71*, 65.

2 Kocarev, L.; Parlitz, U. *Phys. Rev. Lett.* **1995**, *74*, 5028.

3 Parlitz, U.; Kocarev, L.; Stojanovski, T.; Preckel, H. *Phys. Rev. E* **1996**, *53*, 4351.

4 Sharma, N.; Poonacha, P. G. *Phys. Rev. E* **1997**, *56*, 1242.

5 Yoshimura, K. *Phys. Rev. E* **1999**, *60*, 1648.

6 Pecora, L. M.; Carroll, T. L. *Phys. Rev. Lett.* **1990**, *64*, 821.

7 Pyrags, K. *Phys. Lett. A* **1992**, *170*, 421.

8 Kapitaniak, T. *Phys. Rev. E* **1994**, *50*, 1642.

9 Lai, Y. C.; Grebogi, C. *Phys. Rev. E* **1993**, *47*, 2357.

10 Liu, Z. H.; Chen, S. G. *Phys. Rev. E* **1997**, *55*, 6651.

11 John, J. K.; Amritkar, R. E. *Phys. Rev. E* **1994**, *49*, 4843.

12 Huberman, B. A.; Lumer, E. *IEEE Trans. Circuits Sys.* **1990**, *37*, 547.

13 Sinha, S.; Ramaswamy, R.; Subba Rao, J. *Physica D* **1990**, *43*, 118.

14 Gyorgyi, L.; Field, R. J. *J. Phys. Chem.* **1991**, *95*, 6594.

15 Turner, J. S.; Roux, J. C.; McCormick, W. D.; Swinney, H. L. *Phys. Lett. A* **1981**, *85*, 9.

16 Dolnik, M.; Epstein, I. R. *Phys. Rev. E* **1996**, *54*, 3361.

17 Wolf, A.; Swift, J. B.; Swinney, H. L.; Vastano, J. A. *Physcia D* **1985**, *16*, 285.

18 Blakely, J. N.; Gauthier, D. J.; Johnson, G.; Carroll, T. L.; Pecora, L. M. *Chaos* **2000**, *10*, 738.

(E0111278 ZHAO, X. J.; ZHENG, G. C.)